Biochemical Pharmacology xxx (2016) xxx–xxx

Contents lists available at ScienceDirect

Biochemical Pharmacology

journal homepage: www.elsevier.com/locate/biochempharm

Carbachol dimers as homobivalent modulators of muscarinic receptors

Rosanna Matucci [a,*], Marta Nesi [a], Maria Vittoria Martino [b], Cristina Bellucci [b], Dina Manetti [b], Elisa Ciuti [a], Angelica Mazzolari [c], Silvia Dei [b], Luca Guandalini [b], Elisabetta Teodori [b], Giulio Vistoli [c], Maria Novella Romanelli [b]

[a] Department of Neuroscience, Psychology, Drug Research and Child's Health, Section of Pharmacology and Toxicology, University of Florence, Viale G. Pieraccini 6, 50139 Firenze, Italy
[b] Department of Neuroscience, Psychology, Drug Research and Child's Health, Section of Pharmaceutical and Nutraceutical Sciences, University of Florence, Via Ugo Schiff 6, 50019 Sesto Fiorentino, Italy
[c] Department of Pharmaceutical Sciences, University of Milan, Via Mangiagalli 25, 20133 Milano, Italy

ARTICLE INFO

Article history:
Received 21 December 2015
Accepted 15 March 2016
Available online xxxx

Chemical compounds studied in this article:
Carbachol chloride (PubChem CID: 5831)
Acetylcholine chloride (PubChem CID: 6060)
Hexamethonium chloride (PubChem CID: 93550)
Gallamine triethiodide (PubChem CID: 6172)
Atropine sulfate (PubChem CID: 64663)

Keywords:
Muscarinic acetylcholine receptor
Carbachol
Bivalent ligand
Allosteric modulation

ABSTRACT

A series of homodimers of the well-known cholinergic agonist carbachol have been synthesized, showing the two agonist units symmetrically connected through a methylene chain of variable length. The new compounds have been tested on the five cloned muscarinic receptors (hM_{1-5}) expressed in CHO cells by means of equilibrium binding studies, showing an increase in affinity by rising the number of methylene units up to 7 and 9. Functional experiments on guinea-pig ileum and assessment of ERK1/2 phosphorylation on hM_1, hM_2 and hM_3 on CHO cells have shown that the new compounds are endowed with muscarinic antagonistic properties. Kinetic binding studies have revealed that some of the tested compounds are able to slow the rate of dissociation of NMS, suggesting a bitopic behavior. Docking simulations, performed on the hM_1 and hM_2 receptors, give a sound rationalization of the experimental data revealing how these compounds are able to interact with both orthosteric and allosteric binding sites depending on the length of their connecting chain.

1. Introduction

Muscarinic acetylcholine receptors are a group of five membrane proteins (M_1–M_5) belonging to class A G-Protein Coupled Receptors (GPCR), involved in a large number of physiological processes. Several drugs targeting these proteins are in clinical use for diseases, such as chronic obstructive pulmonary disease, overactive bladder and Sjögren's syndrome, but muscarinic modulators may be potentially useful in several other disorders, inside and outside the central nervous system [1,2].

So far the main problem in the development of muscarinic modulators is the high homology found in the M_1–M_5 orthosteric binding site. This has hampered the development of drugs such as xanomeline, a muscarinic agonist potentially useful for Alzheimer's disease or schizophrenia, whose activity was associated to many adverse effects arising from lack of selectivity [3,4]. The discovery of allosteric modulators has opened a new avenue in the development of selective drugs, since these compounds interact with sites which are less conserved within the five muscarinic receptors, thus allowing a selective modulation of only one subtype [5,6].

New intriguing perspectives have been associated also to the discovery of dualsteric (bitopic) ligands, i.e. divalent compounds in which two pharmacophoric units, connected by a suitable spacer, are able to interact at the same time both with the orthosteric site and allosteric binding areas, thus exploiting the favorable characteristics of both sites [7–10]. Originally divalent ligands have been designed to study receptor dimerization [11], but in many instances the length of the linker allowed only the bridging of two neighboring interaction sites on the same protein [9]. Several examples of dualsteric molecules have been reported in the literature, showing interesting properties in terms of subtype selectivity,

* Corresponding author.
E-mail address: rosanna.matucci@unifi.it (R. Matucci).

http://dx.doi.org/10.1016/j.bcp.2016.03.012
0006-2952/

such as THRX-160209 [12], or biased signaling, such as iper-8-naph [13]. In principle, bitopic ligands may interact with the othosteric or the allosteric binding site, or with both, within a monomeric receptor [8]; very recently it has been shown a bitopic interaction also within a dimeric receptor [14].

Several muscarinic homodivalent ligands, i.e. divalent compounds carrying two identical pharmacophoric units, have also been disclosed, such as the M_2 selective antagonist methoctramine [15,16] or the dimers of agonists such as xanomeline [17,18] or arecaidine propargyl ester (APE) [19]. These compounds displayed a different range of potency, affinity and intrinsic activity, depending on the pharmacophoric structure and the linker, as the pharmacophoric doubling did not always result in an increased affinity or potency. In addition, homo or heterobivalent ligands carrying at least one agonist unit were not always endowed with receptor activation properties (see, for instance, Refs. [20,21]).

On this basis we thought it interesting to see the effect of homodimerization on carbachol, the well-known cholinergic agonist: the idea underlying this approach was the possibility to bind two different sites in the same receptor, either orthosteric and allosteric, or two orthosteric sites in a dimeric receptor. Although carbachol itself does not display allosteric properties, the allosteric site of muscarinic receptors can bind compounds carrying choline residues: gallamine is an important example. Therefore, we designed a series of compounds where the two agonist units are symmetrically connected through a methylene chain of variable length, linking the carbamic nitrogen atoms (general formula A, compounds **1a–f**, **2a–f**, Fig. 1A), with the aim to find the optimal length of the spacer; both tertiary amines and ammonium derivatives were prepared. At first, compounds **1a–e** and **2a–e** were synthesized, showing an odd number of carbon units (i.e. n = 3, 5, 7, 9, 11; Fig. 1A); later also compounds **1f** and **2f** (n = 6) were prepared. To check the importance of the second pharmacophoric unit, 2-(dimethylamino)ethyl undecylcarbamate **3** and its quaternary ammonium derivative **4** have been also synthesized and tested. The compounds were tested for their muscarinic activity in binding and functional studies; the results have been rationalized by means of computational methods.

2. Material and methods

2.1. Drugs

The following drugs were used: Carbachol chloride, Acetylcholine chloride, Hexamethonium chloride, Gallamine triethiodide, Atropine sulfate salt monohydrate and (−)-Scopolamine methylbromide were purchased from Sigma–Aldrich SRL, Milano, Italy; [^{3}H]N-methylscopolamine chloride specific activity range 2590–3200 GBq/mmol from Perkin-Elmer Life and Analytical Science, Monza, Milano, Italy. All other test compounds were purchased from Sigma–Aldrich SRL (Milano, Italy) unless stated otherwise.

2.2. Reagents and synthetic methods

All chemicals were of the highest quality commercially available. All melting points were taken on a Büchi apparatus and are uncorrected (Büchi Italia, Milano, Italy). NMR spectra were recorded on a Brucker Avance 400 spectrometer (400 MHz for ^{1}H NMR, 100 MHz for ^{13}C) (Brucker Italia SRL, Milano, Italy). Chromatographic separations were performed on a silica gel column by gravity chromatography (Kieselgel 40, 0.063–0.200 mm; Merck KGaA, Darmstadt, Germany) or flash chromatography (Kieselgel 40, 0.040–0.063 mm; Merck). Yields are given after purification, unless differently stated. When reactions were performed under anhydrous conditions, the mixtures were maintained under nitrogen atmosphere. Compounds were named following IUPAC rules as applied by Reaxys software (www.reaxys.com). In the ^{1}H NMR spectra the following abbreviations are used: s, singlet; bs, broad singlet; d, doublet; t, triplet; q, quartet; m, multiplet.

2.2.1. General procedures for the synthesis of bis(2-(dimethylamino) ethyl)-alkane-α,ω-diyldicarbamate (**1a–f**) and 2-(dimethylamino) ethyl undecylcarbamate **3**

The suitable dicarboxylic acid (n = 5, 7, 9, 11, Fig. 1; 1.5 mmol) was dissolved in CH_2Cl_2 (15 ml) and $SOCl_2$ (15 mmol) was added; the mixture was left stirring at room temperature until it became clear. The solvent was removed under vacuum, then the residue was treated with hexane and the solvent removed again: this step was repeated three times. The residue was dissolved in acetone (4 mL) and treated with a saturated solution of NaN_3 (2 ml); after 0.5 h stirring at room temperature, the mixture is diluted with H_2O and extracted three times with CH_2Cl_2 (10 ml). Drying (Na_2SO_4) and removal of the solvent gave a residue which was dissolved in toluene (12 ml) and heated to reflux for 4 h; after this time the transformation of the acyl azide (IR: 2135 cm^{-1}, N_3) into isocyanate (IR: 2275 cm^{-1}, NCO) was complete. The isocyanate [22] was not isolated; after cooling, dimethylaminoethanol (3 mmol) was added and the solution was first heated at 60 °C for 4 h then left stirring at room temperature overnight. The solvent was removed under vacuum leaving a residue which was

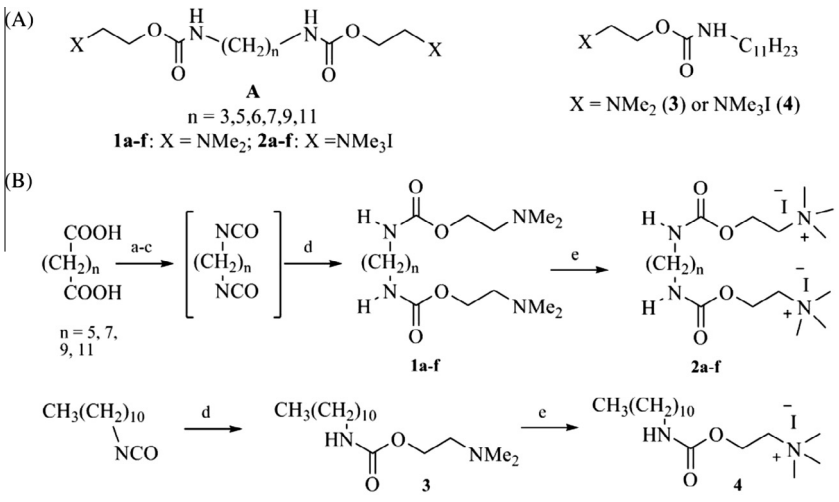

Fig. 1. (A) Chemical structure of the new compounds synthesized in this work; n = 3 (a), 5 (b), 7 (c), 9 (d), 11 (e), 6 (f) (see also Table 1). (B) Synthetic pathway to obtain compounds **1a–f**, **2a–f**, **3** and **4**. Reagents and conditions: (a) $SOCl_2$; (b) NaN_3, acetone; (c) heating, toluene; (d) $Me_2NCH_2CH_2OH$; (e) MeI.

Please cite this article in press as: R. Matucci et al., Carbachol dimers as homobivalent modulators of muscarinic receptors, Biochem. Pharmacol. (2016), http://dx.doi.org/10.1016/j.bcp.2016.03.012

dissolved in diethyl ether and filtered. Removal of solvent gave the desired product, which was purified by flash chromatography, using abs. EtOH/CH_2Cl_2/pet. Ether/NH_4OH 65:340:60:8 as eluent. The reaction with dimethylaminoethanol was performed also on 1,3-diisocyanatopropane ($n = 3$), prepared according to King [23], and on the commercially-available 1,6-diisocyanatohexane ($n = 6$) and 1-undecane isocyanate. The following compounds were prepared.

bis-(2-(Dimethylamino)ethyl)-propane-1,3-diyldicarbamate **1a**: oil; yields: 30%. **[^{1}H] NMR** ($CDCl_3$) δ: 1.58 (quintet, $J = 6.2$ Hz, 2H, CH_2CH_2NH); 2.22 (s, 12H, $4CH_3$); 2.49 (t, $J = 5.6$ Hz, 4H, CH_2N); 3.15 (q, 4H, $J = 6.2$ Hz, CH_2NH); 4.08 (t, $J = 5.6$ Hz, 4H, CH_2O); 5.36 (s, 2H, NH) ppm. **[^{13}C] NMR** ($CDCl_3$, APT) δ: 30.28, 37.65 (CH_2); 45.08 (CH_3); 58.07 (CH_2); 61.9 (CH_2); 156.81 (CO) ppm. Anal. ($C_{13}H_{28}N_4O_4$); calcd: C 51.30, H 9.27, N 18.41; found: C 50.96, H 8.94, N 18.08.

bis-(2-(Dimethylamino)ethyl)-pentane-1,3-diyldicarbamate **1b**: oil; yields: 23%. **[^{1}H] NMR** ($CDCl_3$) δ: 1.34–1.37 (m, 2H, $CH_2CH_2CH_2NH$); 1.47–1.52 (m, 4H, CH_2CH_2NH); 2.46 (s, 12H, $4CH_3$); 2.76 (t, $J = 5.2$ Hz, 4H, CH_2N); 3.14–3.18 (m, 4H, CH_2NH); 4.23 (t, $J = 5.2$ Hz, 4H, CH_2O); 5.25 (s, 2H, NH) ppm. **[^{13}C] NMR** ($CDCl_3$, APT) δ: 23.68, 29.43 40.67 (CH_2); 45.03 (CH_3); 59.08 (CH_2); 61.73 (CH_2); 156.48 (CO) ppm. Anal. ($C_{15}H_{32}N_4O_4$); calcd: C 54.19, H 9.70, N 16.85; found: C 53.85, H 9.34, N 16.51.

bis-(2-(Dimethylamino)ethyl)-heptane-1,3-diyldicarbamate **1c**: Oil; yields: 22%. **[^{1}H] NMR** ($CDCl_3$) δ: 1.27–1.31 (m, 6H, $3CH_2$); 1.47–1.49 (m, 4H, CH_2CH_2NH); 2.54 (s, 12H, $4CH_3$); 2.86 (t, $J = 5.2$ Hz, 4H, CH_2N); 3.12–3.17 (m, 4H, CH_2NH); 4.27 (t, $J = 5.2$ Hz, 4H, CH_2O); 5.31 (s, 2H, NH) ppm. **[^{13}C] NMR** ($CDCl_3$, APT) δ: 26.47, 28.72, 29.70 40.81 (CH_2); 45.36 (CH_3); 58.10 (CH_2); 61.7 (CH_2); 156.40 (CO) ppm. Anal. ($C_{17}H_{36}N_4O_4$); calcd: C 56.64, H 10.07, N 15.54; found: C 56.27, H 9.76, N 15.20.

bis (2-(Dimethylamino)ethyl)-nonane-1,3-diyldicarbamate **1d**: low melting solid; yields: 22%. **[^{1}H] NMR** ($CDCl_3$) δ: 1.18–1.24 (m, 10H, $5CH_2$); 1.40–1.43 (m, 4H, CH_2CH_2NH); 2.25 (s, 12H, $4CH_3$); 2.52 (t, $J = 5.2$ Hz, 4H, CH_2N); 3.09–3.13 (m, 4H, CH_2NH); 4.08–4.13 (m, 4H, CH_2O); 4.85 (s, 2H, NH) ppm. **[^{13}C] NMR** ($CDCl_3$, APT) δ: 26.66, 29.13, 29.35, 40.99 (CH_2); 45.52 (CH_3); 58.25 (CH_2); 61.94 (CH_2); 156.60 (CO) ppm. Anal. ($C_{19}H_{40}N_4O_4$); calcd: C 58.73, H 10.38, N 14.42; found: C 58.39, H 10.02, N 14.47.

bis (2-(Dimethylamino)ethyl)-undecane-1,3-diyldicarbamate **1e**: solid, m.p. 87–89 °C. Yields: 46%. **[^{1}H] NMR** ($CDCl_3$) δ: 1.20–1.24 (m, 14H, $7CH_2$); 1.43–1.46 (m, 4H, CH_2CH_2NH); 2.26 (s, 12H, $4CH_3$); 2.52 (t, 4H, $J = 5.4$ Hz, CH_2N); 3.05–3.13 (m, 4H, CH_2NH); 4.12 (t, 4H, $J = 5.4$ Hz, CH_2O; 4–93 (bs, 1H, NH); 5.63 (bs, 1H, NH) ppm. **[^{13}C] NMR** ($CDCl_3$, APT) δ: 25.44, 26.62, 29.11, 29.16, 29.29, 29.40, 29.81, 35.86, 40.96 (CH_2); 45.44 (CH_3); 58.18 (CH_2); 61.86 (CH_2); 156.6 (CO) ppm. Anal. ($C_{21}H_{44}N_4O_4$); calcd: C 60.54, H 10.65, N 13.45; found: C 60.22, H 10.31, N 13.10.

bis-(2-(Dimethylamino)ethyl)-hexane-1,3-diyldicarbamate **1f** [24]: solid, m.p. 73–75 °C. Yields 87%. **[^{1}H] NMR** ($CDCl_3$) δ: 1.30–1.36 (m, 4H, $CH_2CH_2CH_2CH_2NH$); 1.46–1.49 (m, 4H, CH_2CH_2NH); 2.29 (s, 12H, $4CH_3$); 2.56 (t, 4H, $J = 5.6$ Hz, CH_2N); 3.12–3.17 (m, 4H, CH_2NH); 4.15 (t, $J = 5.6$ Hz, 4H, CH_2O); 4.92 (s, 2H, NH) ppm. **[^{13}C] NMR** ($CDCl_3$) δ: 26.43, 29.91, 41.82 (CH_2); 45.65 (CH_3); 58.43 (CH_2); 58.91 (CH_2); 155.94 (CO) ppm. Anal. ($C_{16}H_{34}N_4O_4$); calcd: C 55.47, H 9.89, N 16.17; found: C 55.52, H 9.63, N 16.01.

2-(Dimethylamino)ethyl undecylcarbamate **3**: hygroscopic solid; yields: 90%. **[^{1}H] NMR** (CD_3Cl_3) δ: 0.87 (t, $J = 6.8$ Hz, 3H, CH_3C); 1.18–1.33 (m, 16H, $8CH_2$); 1.45–1.49 (m, 2H, CH_2CH_2NH); 2.30 (s, 6H, CH_3N); 2.55 (t, $J = 5.4$ Hz, 2H, CH_2N); 3.13–3.18 (m, 2H, CH_2NH); 4.16 (t, $J = 5.4$ Hz, 2H, CH_2O); 4.81 (bs, 1H, NH) ppm. **[^{13}C] NMR** (CD_3Cl_3, APT) δ (ppm): 14.09 (CH_3); 22.67, 26.75, 29.31. 31.89, 41.06 (CH_2); 45.48 (CH_3N); 58.25 (CH_2); 61.88 (CH_2); 155.9 (CO) ppm. Anal. ($C_{16}H_{34}N_2O_2$); calcd: C 67.09, H 11.96, N 9.78; found: C 67.29, H 11.80, N 9.95.

2.2.2. General procedure for the synthesis of methiodides

An excess of CH_3I was added to a solution of the suitable amine (**1a–f**, **3**) dissolved in anhydrous diethyl ether (30 ml each mmol of reagent). The mixture was left stirring at room temperature overnight in the dark. The solid was collected and dried. By this way the following compounds were prepared.

bis-(2-(Dimethylamino)ethyl)-propane-1,3-diyldicarbamate methiodide **2a**: solid, m.p. 168–170 °C. Yields: 50%. **[^{1}H] NMR** (CD_3OD) δ: 1.69 (quintet, $J = 6.8$ Hz, 2H, CH_2CH_2NH,); 3.18 (t, $J = 6.8$ Hz, 4H, CH_2NH); 3.22 (s, 18H, $6CH_3$); 3.70–3.73 (m, 4H, CH_2N); 4.50–4.52 (m, 4H, CH_2O) ppm. **[^{13}C] NMR** (CD_3OD, APT) δ: 29.27, 37.32 (CH_2); 53.21 (CH_3); 57.86 (CH_2); 65.22 (CH_2); 155.90 (CO) ppm. Anal. ($C_{15}H_{34}I_2N_4O_4$); calcd: C 30.63, H 5.83, N 9.52; found: C 30.32, H 5.46, N 9.43.

bis-(2-(Dimethylamino)ethyl)-pentane-1,3-diyldicarbamate methiodide **2b**: hygroscopic solid. Yields: 20%. **[^{1}H] NMR** (CD_3OD) δ: 1.36–1.39 (m, 2H, $CH_2CH_2CH_2NH$); 1.59–1.49 (m, 4H, CH_2CH_2NH,); 3.12 (t, 4H, $J = 6.8$ Hz, CH_2NH); 3.24 (s, 18H, $6CH_3$); 3.70–3.72 (m, 4H, CH_2N); 4.48–4.52 (m, 4H, CH_2O) ppm. **[^{13}C] NMR** (CD_3OD, APT) δ: 23.61, 29.06, 40.40 (CH_2); 53.27 (CH_3); 53.31 (CH_3); 57.76 (CH_2); 65.23 (CH_2); 156.50 (CO) ppm. Anal. ($C_{17}H_{38}I_2N_4O_4$); calcd: C 33.13, H 6.21, N 9.09; found: C 32.98, H 6.54, N 9.37.

bis-(2-(Dimethylamino)ethyl)-heptane-1,3-diyldicarbamate methiodide **2c** [25]: hygroscopic solid. Yields: 87%. **[^{1}H] NMR** (CD_3OD) δ: 1.32–1.35 (m, 6H, $3CH_2$); 1.49–1.53 (m, 4H, CH_2CH_2NH); 3.11 (t, $J = 6.8$ Hz, 4H, CH_2NH); 3.26 (s, 18H, $6CH_3$); 3.73–3.75 (m, 4H, CH_2N); 4.50–4.52 (m, 4H, CH_2O) ppm. **[^{13}C] NMR** (CD_3OD, APT) δ: 26.33, 28.60, 29.30, 40.49 (CH_2); 53.41 (CH_3); 57.83 (CH_2); 65.25 (CH_2); 156.03 (CO) ppm. Anal. ($C_{19}H_{42}I_2N_4O_4$); calcd: C 35.41, H 6.57, N 8.69; found: C 35.09, H 6.44, N 8.82.

bis-(2-(Dimethylamino)ethyl)-nonane-1,3-diyldicarbamate methiodide **2d**: solid, m.p. 80–82 °C. Yields: 26%. **[^{1}H] NMR** (CD_3OD) δ: 1.24–1.31 (m, 10H, $5CH_2$); 1.46–1.51 (m, 4H, CH_2CH_2NH); 3.09 (t, 4H, $J = 6.8$ Hz, CH_2NH); 3.22 (s, 18H, $6CH_3$); 3.65–3.70 (m, 4H, CH_2N); 4.37–4.50 (m, 4H, CH_2O) ppm. **[^{13}C] NMR** (CD_3OD, APT) δ: 26.41, 28.91, 29.16, 29.40, 40.53 (CH_2); 53.41 (CH_3); 57.81 (CH_2O); 65.25 (CH_2N); 156.50 (CO) ppm. Anal. ($C_{21}H_{46}I_2N_4O_4$); calcd: C 37.51, H 6.90, N 8.33; found: C 37.88, H 6.72, N 8.56.

bis-(2-(Dimethylamino)ethyl)-undecane-1,3-diyldicarbamate methiodide **2e**: solid, m.p. 106–108 °C. Yields: 34%. **[^{1}H] NMR** (CD_3OD) δ: 1.26–1.35 (m, 14H, $7CH_2$); 1.48–1.53 (m, 4H, CH_2CH_2NH,); 3.09 (t, 4H, $J = 6.8$ Hz, CH_2NH); 3.22 (s, 18H, $6CH_3$); 3.67–3.70 (m, 4H, CH_2N); 4.45–4.50 (m, 4H, CH_2O) ppm. **[^{13}C] NMR** (CD_3OD) δ: 26.41, 28.91, 29.16 (CH_2); 29.40 (CH_2CH_2NH); 40.53 (CH_2NH); 53.41 (CH_3); 57.81 (CH_2O); 65.25 (CH_2N); 156.43 (CO) ppm. Anal. ($C_{23}H_{50}I_2N_4O_4$); calcd: C 39.44, H 7.19, N 8.00; found: C 39.51, H 6.87, N 8.24.

bis-(2-(Dimethylamino)ethyl)-hexane-1,3-diyldicarbamate methiodide **2f** [24,25]: solid, m.p. 178–180 °C. Yields: 28%. **[^{1}H] NMR** (CD_3OD) δ: 1.33–1.36 (m, 4H, $2CH_2$); 1.49–1.53 (m, 4H, CH_2CH_2NH,); 3.11 (t, $J = 6.8$ Hz, 4H, CH_2NH); 3.26 (s, 18H, $6CH_3$); 3.73–3.75 (m, 4H, CH_2N); 4.50–4.52 (m, 4H, CH_2O) ppm. **[^{13}C] NMR** (CD_3OD, APT) δ: 25.98, 29.28, 40.36 (CH_2); 53.4 (CH_3); 57.8 (CH_2); 65.3 (CH_2); 156.0 (CO) ppm. Anal. ($C_{18}H_{40}I_2N_4O_4$); calcd: C 34.30, H 6.40, N 8.89; found: C 33.98, H 6.56, N 8.50.

2-(Dimethylamino)ethyl undecylcarbamate methiodide **4**: white solid, m.p. 86–88 °C. Yields: 70%. **[^{1}H] NMR** (CD_3OD) δ: 0.90 (t, $J = 6.8$ Hz, 3H, CH_3); 1.16–1.29 (m, 16H, $8CH_2$); 1.48–1.50 (m, 2H, CH_2CH_2NH); 3.10 (t, $J = 7.0$, 2H, CH_2NH); 3.21 (s, 9H, CH_3N); 3.66–3.68 (m, 2H, CH_2N); 4.50 (m, 2H, CH_2O) ppm. **[^{13}C] NMR** (CD_3OD, APT) δ: 13.05 (CH_3); 22.33, 26.48, 29.33, 31.66, 40.56 (CH_2); 53.35 (CH_3N); 57.8 (CH_2); 65.3 (CH_2); 155.89 (CO) ppm. Anal. ($C_{17}H_{37}IN_2O_2$); calcd: C 47.66, H 8.71, N 6.54; found: C 47.42, H 8.77, N 6.33.

Please cite this article in press as: R. Matucci et al., Carbachol dimers as homobivalent modulators of muscarinic receptors, Biochem. Pharmacol. (2016), http://dx.doi.org/10.1016/j.bcp.2016.03.012

2.3. Binding assays

2.3.1. Cell culture and membrane preparation

Chinese Hamster Ovary (CHO) cells stably expressing the human muscarinic receptors (hM_1–hM_5) were routinely cultured in Dulbecco's Modified Eagle Medium (DMEM) supplemented with 10% fetal bovine serum (FBS), 100 units/ml each of penicillin G and streptomycin, 4 mM glutamine (Sigma–Aldrich, Milano, Italy), non-essential aminoacid solution 100x (Sigma–Aldrich, Milano, Italy) and 50 μg/ml of geneticin (Gibco, Grand Iland, NY).

Membrane preparations were conducted as described previously [26]. Briefly, confluent CHO cell lines were scraped, washed with PBS buffer (25 mM sodium phosphate, containing 5 mM $MgCl_2$ at pH 7.4) and homogenized for 30 s using an Ultra-Turrax (setting 5) (IKA-Werke GmbH & Co. KG, Staufen, Germany). The pellet was sedimented 17,000*g* for 15 min at 4 °C and the membranes were resuspended in the same buffer, re-homogenized with Ultra-Turrax and stored at 80 °C. The protein content was measured according to the method of Bradford [27] using the Bio-Rad protein assay reagent (Bio-Rad Laboratories, Munchen, Germany).

2.3.2. Equilibrium radioligand binding assays

Radioligand equilibrium binding experiments with membrane homogenates from CHO cells expressing one of the five muscarinic subtypes were conducted in a 25 mM PBS containing 5 mM $MgCl_2$ at pH 7.4, at room temperature as described previously [26]. Briefly, membranes (25–70 μg/ml) were incubated with 0.2 nM [^{3}H]N-methylscopolamine chloride ([^{3}H]NMS) and different concentrations (usually 0.1 nM–1000 μM) of unlabeled test compounds in PBS buffer plus $MgCl_2$ in polypropylene 96-well plates (Sarstedt, Verona, Italy) in a final volume of 0.25 ml for 2 h.

At the end of the binding reaction, free radioligand was separated from bounded ligand by rapid filtration through UniFilter GF/C plates (Perkin-Elmer Life and Analytical Science, Monza, Italy) using a FilterMate Cell Harvester (Perkin-Elmer Life and Analytical Science, Monza, Italy). After filtration, the filters were washed several times with ice-cold milliQ water and dried at room temperature under air flow. 25 μl of scintillation liquid Microscint 20 (Perkin-Elmer Life and Analytical Science, Monza, Italy) was added to each well and the quantity of membrane-bound radioligand was measured by TopCount NXT Microplate Scintillation Counter (Perkin-Elmer Life and Analytical Science, Monza, Italy) after 4 h.

Stock solutions of tested compounds were made in DMSO, and dilutions were usually made in the incubation buffer. DMSO at the highest concentration used (10%) had no effect on binding. In all radioligand binding assays nonspecific binding was defined using 10 μM atropine. In all assays, the total binding was always less than 10% of the total counts added.

2.3.3. Dissociation kinetic assays

2.3.3.1. Full time course. For these experiments, a high concentration of CHO cell membranes (50–100 μg/ml) was equilibrated with 2 nM [^{3}H]NMS in PBS buffer for 60 min at room temperature. Then, 100 μl aliquots of this mixture were distributed into tubes, which contained 10 μl of 100 μM atropine to prevent radioligand reassociation to receptors (final total volume 1 ml), at various time points (0, 1, 10, 20, 40, 80 and 160 min). At the appropriate time, samples were filtered. Incubation was terminated by rapid filtration through Whatman GF/C filters (Brandel, Gaithersburg, MD, USA), that had been presoaked in a 0.05% polyethylenimine (PEI) solution for at least 1 h, using a Brandell cell harvester (Biomedical Research and Development Laboratory, Inc Atlas Drive, Gaithersburg, MD, USA). Filters were washed three times with 3 ml aliquots of ice-cold milliQ water and dried before the addition of 4.5 ml of scintillation cocktail (Filter Count, Perkin-Elmer Life and Analytical Science, Monza, Italy). The radioactivity was determined using scintillation counting (TRI-CARB 1100, Perkin-Elmer Life and Analytical Science, Monza, Italy). The determination of nonspecific binding, the filtration method and the counting procedure were the same in all the [^{3}H]NMS dissociation kinetic assays described subsequently in this section.

2.3.3.2. One point kinetic assays. Off-rate assays were performed to estimate the affinity of compounds **1b**–**f**, **2b**–**f**, **3**, **4** and gallamine for the [^{3}H]NMS occupied receptor. In subsequent experiments, designed to investigate the effects of a range of modulator concentrations on the [^{3}H]NMS dissociation rate, a "one point kinetic assay" approach was used, where the effect on radioligand dissociation of each test ligand was determined at 0 min and at one time point, which was chosen to be ca 2.5 dissociation half-lives of [^{3}H]NMS alone [28]. A high concentration of hM_1–hM_5 CHO membranes (50–75 μg/ml) was incubated with a high concentration of [^{3}H]NMS (2 nM) for about 60 min at room temperature. Then, 100 μl aliquots were distributed into tubes which contained 10 μl of 100 μM atropine alone, or in the presence of different concentrations of test compounds, and diluted in 1 ml total volume of buffer. The time zero data point was obtained using only 100 μl of the mixture containing membranes plus [^{3}H]NMS. At a fixed time point later (80 min for hM_1, 20 min for hM_2, 100 min for hM_3, 90 min for hM_4, 70 min for hM_5) the samples were filtered as described above.

2.4. Functional assays

2.4.1. Guinea-pig ileum

This preparation was set up according to Dei [26] on guinea pig ileum. The terminal portion of ileum was taken at about 1.5 cm from the ileum–cecum junction from male guinea-pigs (200–300 g); segments 2 cm in length were carefully removed, washed and then mounted isotonically under a tension of 0.5 g in 10 ml organ baths filled with Krebs–Henseleit solution (composition mM: NaCl 118.0, KCl 4.7, $CaCl_2$ 2.52, KH_2PO_4 1.18, $MgSO_4.7H_2O$ 1.18, $NaHCO_3$ 25.0 and glucose 11.1), gassed with 95% O_2: 5%CO_2 and maintained at 37 °C.

After one hour to allow for equilibration, non-cumulative concentration–response curves to carbachol (CCh), acetylcholine (ACh) and the new compounds were constructed. The tissues were exposed to drugs for 30 s until maximum contraction was reached and then washed. The contractions were recorded by means of a force displacement transducer (Ugo Basile SRL, Varese, Italy) connected to the recorder Unirecord 7050 (Ugo Basile SRL, Varese, Italy).

The responsiveness of each piece of tissue was assessed by considering the responses to the same concentration of ACh or CCh at the beginning and end of the experiment. Agonist efficacy (expressed as $pD_2 = -\log EC_{50}$) and maximum response were determined.

When the compounds were tested as antagonists, a dose–response curve to the agonists ACh was repeated after 45 min incubation with the test compounds (1 μM). Antagonist potency was expressed as pK_B (for the definition of pK_B see Section 2.6.2).

All animal experiments were conducted in accordance with the principles for the care and use of laboratory animals for scientific purposes contained in the European Union regulations (Directive 2010/63/EU).

2.4.2. Extracellular Signal-Regulated Kinase (ERK1/2) Phosphorylation Assays

These assays were performed using the Cellul'ERK kit (Cisbio Bioassays, Codolet, France). CHO cells stably transfected with the human muscarinic receptors (M_1–M_3) were plated into 96-well plates (Sarstedt, Verona, Italy) at a density of 40,000 cells/well and grown for at least 4 h in DMEM medium containing 10% FBS,

Please cite this article in press as: R. Matucci et al., Carbachol dimers as homobivalent modulators of muscarinic receptors, Biochem. Pharmacol. (2016), http://dx.doi.org/10.1016/j.bcp.2016.03.012

100 U/ml penicillin, and 100 μg/ml streptomycin, with L-glutamine as required for the cell line used. Cells were then washed twice with PBS and were starved by replacing the cell growth media with similar media that did not contain FBS and incubating at 37 °C overnight to allow FBS-stimulated phosphorylated ERK1/2 levels to subside.

For stimulation experiments, agonists were diluted into FBS-free media and applied to the cells for 5–8 min. For inhibition experiments, a similar protocol was followed, but the cells were preincubated with the inhibitor for 30 min prior to stimulation.

The Cellul'ERK kit assay was performed in accordance with the manufacturer's instructions, using only reagents supplied with the kit. Briefly, media containing the compounds were removed from 96-well plates, 50 μl of lysis buffer was added to the wells and the plates were incubated for 30 min at room temperature with shaking to lyse the cells.

Lysate mixture (16 μl) was transferred to a 384-well Proxiplate (Perkin-Elmer Life and Analytical Science, Monza, Italy), then conjugate working solution (4 μl) was added and the plate was sealed, wrapped in metal foil to shield from light, and incubated for 2 h at room temperature. The fluorescence signal in the wells was determined with a Flex Station 3 Microplate Reader (Molecular Devices, Sunnyvale, CA, USA).

All data were expressed as a percentage of ERK1/2 phosphorylation produced after a 5 min exposure to Dulbecco's modified Eagle's medium containing 10% FBS.

2.5. Computational studies

Docking simulations involved the recently resolved structures of the hM_2 subtype in complex with both the agonist iperoxo and the allosteric modulator LY2119620 (PDB Id: 4MQT) as well as in complex with the antagonists QNB (PDB Id: 3UON). The choice of the first hM_2 structure is justified by the bound ligands which should assure that both binding cavities (allosteric and orthosteric sites) are finely optimized for ligand recognition. The second hM_2 structure was selected to simulate receptor conditions similar to those experienced during the kinetic experiments. Again, docking studies involved the hM_1 (Entry Id: P11229, Entry name: ACM1_HUMAN) homology model as generated using the first hM_2 structure as the template. Briefly, the homology modeling was performed by Modeller 9.10 using the default parameters [29]; among the 20 generated models, the best structure was selected according to the computed scores (i.e. DOPE and GA341) as well as to the percentage of residues falling in the allowed regions of the Ramachandran (91.2%) and chi plots (95.8%). The completed model was carefully checked to avoid unphysical occurrences such as cis peptide bonds, wrong configurations, improper bond lengths, non-planar aromatic rings or colliding side-chains.

The so obtained hM_1 and hM_2 structures were then completed by adding hydrogen atoms and to remain compatible with physiological pH, Asp, Glu, Lys and Arg residues were considered in their ionized form while His and Cys were maintained neutral by default. Finally, the structures were optimized by a minimization made up by two phases: a first minimization without constraints until RMS = 0.1 kcal mol^{-1} $Å^{-1}$ and then a second minimization with backbone fixed until RMS = 0.01 kcal mol^{-1} $Å^{-1}$ to preserve their folding.

All ligands were simulated in their protonated state since this is involved in receptor recognition. The conformational profile was investigated by MonteCarlo simulations (as implemented in the VEGA program [30], which produced 1000 minimized conformations by randomly rotating the rotatable bonds and the so computed lowest energy structure underwent docking simulations.

Docking simulations were carried out using PLANTS [31] with default settings and without geometric constraints. The search within the first hM_2 structure and the hM_1 homology model was focused on a region obtained combining a 10.0 Å radius sphere around Asp105 (hM_1) or Asp103 (hM_2) plus a 10.0 Å radius sphere around Tyr179 (hM_1) or Tyr177 (hM_2) thus completely encompassing both binding cavities. In contrast, the search within the second hM_2 structure was focused on a region obtained combining a 10.0 Å radius sphere around Tyr177 keeping the bound QNB antagonist. For each ligand, speed 1 was used and 10 poses were generated and scored using the ChemPlp function. The so obtained best complexes were finally optimized by a minimization keeping all atoms fixed apart from those included within a 10.0 Å radius sphere around the bound ligand.

2.6. Data analysis

2.6.1. Binding assays

Data are presented as mean ± S.E.M., unless otherwise noted. Data from equilibrium binding studies were corrected for non specific binding and were analyzed by computer-aided nonlinear regression analysis using a four parameter logistic equation in GraphPad Prism 5.02 (GraphPad Software, San Diego, CA). IC_{50} values were, irrespective of the slope factor of the curve, converted to binding constants K_i using the Cheng–Prusoff correction.

Radioligand dissociation rates were analyzed by nonlinear regression according to the following equation for monoexponential decay using GraphPad Prism 5.02:

$$Y = Y_0 \times \exp(-k \times X) + \text{Plateau} \quad (1)$$

where Y_0 is the specific binding of the radioligand at time = 0, before dissociation was initiated. Y is bound radioligand (specific binding) after dissociation for time X. The equation starts at (Y_0 + Plateau) at time = 0 and decays to Plateau with a rate constant k. The half-life is 0.69/k. k is the k_{off} and denotes the observed radioligand dissociation rate constant in the absence or presence (k_{offobs}) of the allosteric modulator. For monoexponential and fully reversible binding it is predicted that the curve would decay to Plateau = 0.

According to the detailed protocol developed by [28], one point kinetic data were analyzed in order to obtain estimates of the affinity of an allosteric agent for the [^{3}H]NMS-occupied receptor (K_{occ}) in a single step. Eq. (1) was modified by substituting k (=k_{offobs}) by:

$$K_{off}/(1 + K_{occ} \times X) \quad (2)$$

where k_{off} is the dissociation rate constant of the radioligand in the absence of X. X refers to the log concentration of the allosteric ligand and $\log K_{occ}$ is its log affinity constant for the occupied receptor. The resulting equation directly gives the values of [^{3}H]NMS rate constants in the absence (k_{off}) and in the presence of allosteric modulators (k_{offobs}) and an estimate of $\log K_{occ}$ by analyzing the amount of [^{3}H]NMS remaining at certain times at different concentrations of the allosteric modulators (see [28]).

2.6.2. Functional assays

Results are given as mean ± SEM of n experiments and a two-tailed Student's t-test was used for comparison of mean values. The agonist concentration–response curves were analyzed using computer GraphPad Prism 5.02 (GraphPad Software, San Diego, CA) that fits the data directly with a logistic function, providing the EC_{50} value (the concentration required for an agonist to produce a half-maximal response: $-\log EC_{50} = pD_2$), the maximum response (E_{max}).

The antagonist potency (pK_B) was estimated using the following Eq. (3) [32] where a single concentration of antagonist was used. Agonist EC_{50} values in the absence and presence of antagonists were determined graphically for the calculation of dose ratios (DR).

$$pK_B = \log(DR - 1) - \log(\text{concentration of antagonist}) \quad (3)$$

3. Results

3.1. Chemistry

Compounds **1a–f** and **3** were obtained by reacting the suitable isocyanate or diisocyanate with dimethylaminoethanol as shown in Fig. 1B. 1,6-Diisocyanatohexane and 1-isocyanatoundecane were commercially available; 1,3-diisocyanatopropane was obtained according to King [23], while the other diisocyanates were prepared from commercially available alkanedicarboxylic acids, which were transformed into the acyl azides by reaction first with thionyl chloride and then with sodium azide in acetone; Curtius rearrangement gave the desired compounds. Reaction of carbamates **1a–f** and **3** with methyl iodide gave the corresponding quaternary ammonium analogs **2a–f** and **4**, respectively.

3.2. [^{3}H]N-methyl scopolamine equilibrium binding studies

The compounds were tested in equilibrium binding studies on membrane preparations from CHO-K1 cells stably expressing the five human muscarinic receptors (hM_1–hM_5), using [^{3}H]NMS as radioligand and carbachol (CCh) as reference [26].

All the compounds displaced, in a concentration-dependent manner, 0.2 nM [^{3}H]NMS from the five mAChRs, with different potency but without subtype selectivity (pK_i values are shown in Table 1).

Compounds **1c–e** and **2c–e** strongly and completely inhibited the binding of 0.2 nM [^{3}H]NMS, while **1a**,**b** and **2a**,**b** fully displaced the radioligand only from some subtypes, even at the highest concentrations tested (1 mM), showing pK_i values <5. As an example, Fig. 2 shows the inhibition curves of the methiodides **2a–e**, measured on hM_1 (Fig. 2A) and hM_2 (Fig. 2B); CCh is used as reference. The hM_3–hM_5 subtypes gave similar graphs (data not shown).

Table 1 shows that affinity is usually higher for methiodides with respect to tertiary amines, although the difference is below one log unit, and increases with the length of the methylene chain up to $n = 7$ or $n = 9$, depending on the receptor subtype or on the amine–ammonium functionality, with a slight decline when $n = 11$; at hM_2 receptor subtype the lowest affinities were revealed.

Interestingly, compounds **1a–e** and **2a–e** can be divided into two groups according to their pK_i values (Fig. 3A and B). The affinity of compounds **1a**,**b** and **2a**,**b** ($n \leqslant 5$) is low, although in the same range as the orthosteric ligand CCh; on the contrary compounds with $n \geqslant 7$ have pK_i values higher than 7 with few exceptions (**1c**, $n = 7$ and **1d**, $n = 9$, on hM_2, and **1e**, $n = 11$ on hM_2, hM_3, hM_4 and hM_5). Actually, two-methylene elongation of the spacer brings about a difference in affinity which is usually below 1 log unit, except when going from $n = 5$–7.

This finding prompted us to synthesize and test the analogs with $n = 6$, **1f** and **2f**, which were found able to fully inhibit the binding of [^{3}H]NMS to hM_1–hM_5 receptors, with pK_i values intermediate between those of the compounds with 5 and 7 methylene units (Table 1).

In order to determine if the second carbachol unit could affect the affinity to muscarinic receptors, compound **3** and its methiodide **4**, carrying on the carbamic nitrogen atom a long but not functionalized alkyl chain, has been prepared and tested: their pK_i values (Table 1) were found in the same range as those of the bivalent compounds with long chain ($n \geqslant 7$). Similarly to their analogs, they were not able to discriminate among receptor subtypes.

3.3. Functional studies

3.3.1. Isolated guinea-pig ileum

Preliminary evaluation of the functional muscarinic properties of compounds **1a–f** and **2a–f** was assessed on isolated guinea pig ileum, a functional model readily available to us, according to an already published protocol [33].

Compounds **1a**,**b**, **2a**,**b** and **2f** ($n = 3$–6) evoked weak smooth muscle contractions, even at the highest concentration tested (100 μM) (Table 1); only **2b** ($n = 5$) and **2f** ($n = 6$) displayed a dose-dependent effect ($pD_2 = 4.93 \pm 0.09$ and $pD_2 = 5.10 \pm 0.10$, respectively, Fig 4A). Compound **1f** ($n = 6$) as well as the higher homologs ($n \geqslant 7$, both amines and methiodides) were totally unable to contract guinea pig smooth muscle preparation.

In order to verify the involvement of the muscarinic system in the agonistic effect of compounds **2b** and **2f**, dose–response curves were performed after 30 min preincubation with atropine 1 nM. While, as expected [34,35], atropine completely inhibited ACh and CCh induced contractions, it failed to significantly modify the contractile response induced by **2b** and **2f**, which, on the contrary, was prevented by pretreatment with 30 μM hexamethonium (data not shown).

Table 1
Equilibrium binding affinity and functional activity of the tested compounds. Inhibition binding constants (pK_i) of the compounds for human cloned muscarinic receptors expressed in CHO-K1 cells membranes. Agonist or antagonist potencies (pD_2 or pK_B, respectively) from functional tests on guinea-pig ileum preparations. Values are reported as mean of 3–4 experiments. n.a. = not active.

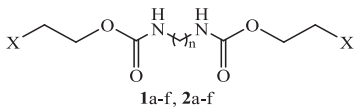

1a-f, **2**a-f

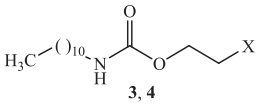

3, **4**

	n	X	hM_1	hM_2	hM_3	hM_4	hM_5	Guinea pig ileum
1a	3	NMe_2	4.68 ± 0.08	4.14 ± 0.08	<4	<4	<4	$pD_2 < 4$
2a	3	NMe_3I	4.91 ± 0.04	4.65 ± 0.04	<4	<4	<4	$pD_2 < 4$
1b	5	NMe_2	4.98 ± 0.11	4.84 ± 0.06	4.46 ± 0.10	4.24 ± 0.08	4.41 ± 0.09	$pD_2 < 4$
2b	5	NMe_3I	4.95 ± 0.07	4.95 ± 0.05	4.79 ± 0.07	<4	4.84 ± 0.07	$pD_2 = 4.93 \pm 0.09$
1c	7	NMe_2	7.45 ± 0.05	6.42 ± 0.07	7.76 ± 0.05	7.27 ± 0.04	8.01 ± 0.05	$pK_B = 5.61 \pm 0.12$
2c	7	NMe_3I	7.75 ± 0.05	7.20 ± 0.05	8.14 ± 0.04	7.70 ± 0.04	8.19 ± 0.03	$pK_B = 6.82 \pm 0.13$
1d	9	NMe_2	7.56 ± 0.05	6.53 ± 0.06	7.89 ± 0.05	7.48 ± 0.04	7.68 ± 0.05	$pK_B = 5.31 \pm 0.08$
2d	9	NMe_3I	7.93 ± 0.03	7.35 ± 0.04	8.02 ± 0.02	7.78 ± 0.05	7.91 ± 0.06	$pK_B = 6.66 \pm 0.05$
1e	11	NMe_2	7.16 ± 0.06	6.29 ± 0.05	6.89 ± 0.04	6.80 ± 0.09	6.76 ± 0.05	$pK_B = 5.33 \pm 0.03$
2e	11	NMe_3I	7.59 ± 0.05	7.38 ± 0.04	7.50 ± 0.04	7.49 ± 0.06	7.35 ± 0.03	$pK_B = 6.67 \pm 0.09$
1f	6	NMe_2	6.18 ± 0.05	5.37 ± 0.03	6.16 ± 0.07	5.78 ± 0.06	6.12 ± 0.06	n.a.
2f	6	NMe_3I	6.16 ± 0.04	5.73 ± 0.03	6.28 ± 0.04	5.87 ± 0.05	6.36 ± 0.05	$pD_2 = 5.10 \pm 0.10$
3	–	NMe_2	7.50 ± 0.04	6.80 ± 0.05	7.34 ± 0.04	7.05 ± 0.03	7.30 ± 0.02	$pK_B = 6.40 \pm 0.10$
4	–	NMe_3I	8.19 ± 0.02	7.73 ± 0.04	7.85 ± 0.05	7.69 ± 0.04	8.00 ± 0.05	$pK_B = 7.41 \pm 0.12$
Carbachol			4.42 ± 0.01	5.92 ± 0.07	4.36 ± 0.01	5.20 ± 0.07	4.16 ± 0.09	$pD_2 = 6.68 \pm 0.01$

Please cite this article in press as: R. Matucci et al., Carbachol dimers as homobivalent modulators of muscarinic receptors, Biochem. Pharmacol. (2016), http://dx.doi.org/10.1016/j.bcp.2016.03.012

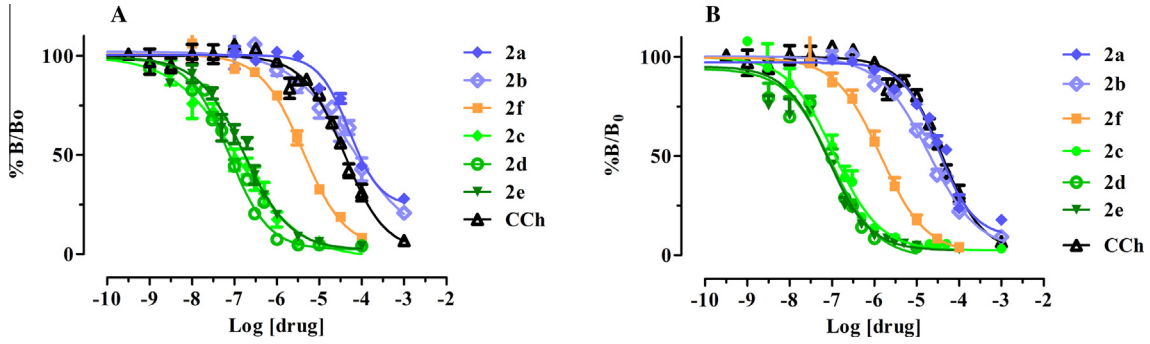

Fig. 2. Inhibition of [^{3}H]NMS specific binding by CCh and **2a–f** in membrane homogenates of CHO cells stably expressing the hM_1 (A) and hM_2 (B) mAChRs. Curves from single experiments were fitted using the standard four parameter logistic equation and are the mean ± S.E.M. from three to six independent experiments.

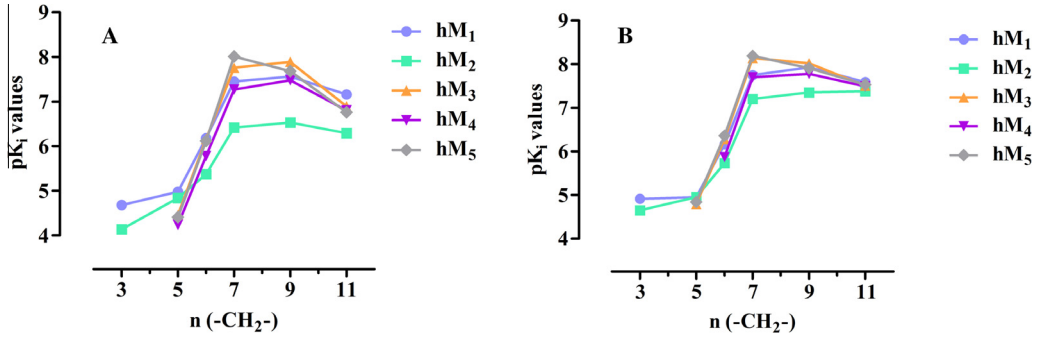

Fig. 3. The pK_i values of compounds **1a–f** (A) and **2a–f** (B) from the equilibrium binding studies are shown as a function of the length of the spacer. Values represent the mean ± S.E.M. from three to six independent experiments and the error bars are smaller than symbols used.

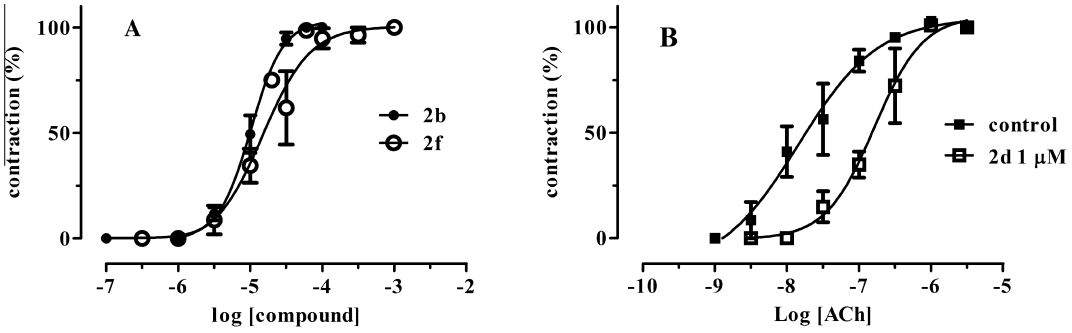

Fig. 4. (A) Concentration–response curve for contractions evoked by **2b** (n = 5) and **2f** (n = 6) in guinea-pig ileum. (B) Inhibition effect of 1 µM **2d** on ACh induced contractions in guinea-pig ileum. The effect is expressed as percentage of the maximum, normalized to the maximum response given by carbachol in the same experiment (100% of contraction). The data points represent the mean ± SEM of 2–4 experiments.

In order to assess the functional behavior of compounds with $n \geqslant 7$, as well as that of **1f**, ACh dose–response curves were conducted in the absence (pD_2 = 7.84 ± 0.26) and in the presence of fixed concentrations of these molecules (1–30 µM). Compounds **1c–e** and **2c–e** behaved as antagonists, shifting rightward the dose–response curves of ACh (a representative dose–response curve is reported in Fig. 4B for **2d**): their potency is reported in Table 1 as pK_B calculated according to the Van Rossum equation [32]. Quaternary ammonium compounds **2c–e** were about one order of magnitude more potent than the corresponding tertiary amines **1c–e**. The pK_B values reported in Table 1 show that the antagonist potency of amines **1c–e** and methiodides **2c–e**-does not depend on the chain length.

In the same test, also N-undecanyl derivatives **3** and **4** behaved as antagonist, as they were able to shift rightward in a parallel way ACh dose–response curves, with and pK_B values of 6.40 ± 0.10 and 7.41 ± 0.12, respectively (Table 1).

Surprisingly, compound **1f**, despite its micromolar affinity assessed in radioligand binding studies, did not show functional activity in this test.

3.3.2. ERK1/2 phosphorylation assays

To further investigate functional activity, avoiding the interference of nicotinic receptors, selected compounds (**2b**, **2c**, **2f**, **4** and **1f**) were evaluated in the ERK1/2 phosphorylation assay in intact CHO cells stably expressing M_1, M_2, and M_3 human mAChRs.

At first, each compound (10–100 µM) was tested alone to assess intrinsic agonism. ACh (10 nM), taken as reference, mediated a robust stimulation of ERK1/2 phosphorylation, that peaked at 5 min in CHO cells and was prevented by preincubation with 10 µM atropine. In contrast, none of the tested compounds stimulated ERK1/2 phosphorylation, failing to elicit a functional response at the hM_1–hM_3 mAChRs (data not shown).

Please cite this article in press as: R. Matucci et al., Carbachol dimers as homobivalent modulators of muscarinic receptors, Biochem. Pharmacol. (2016), http://dx.doi.org/10.1016/j.bcp.2016.03.012

Given the lack of agonist activity of these compounds, we investigated their antagonist properties toward ACh. The compounds were preincubated for 30 min at 100 μM before adding ACh 10 nM [36]. Fig. 5 shows the results on hM_1 receptors: **2c** and **4** confirmed the antagonistic behavior shown on guinea-pig ileum (Table 1), completely preventing ACh-induced ERK1/2 phosphorylation (comparable effect to that of atropine); **2b**, **2f** and also **1f** showed a significant reduction. Analogous results were found also in hM_2 and hM_3 receptor subtypes (data not shown), pointing to a muscarinic antagonistic profile of this class of compounds.

3.4. Kinetic binding studies

To study the potential interactions of this series of molecules with a secondary site on muscarinic receptors, kinetic binding experiments were performed. Since it is known that ligands that bind to a secondary (allosteric) site on GPCRs modify the dissociation rate of the ligand bound to the primary (orthosteric) site [7], the ability of the tested compounds to affect [^{3}H]NMS dissociation rate was investigated.

To determine the time course of [^{3}H]NMS dissociation, preliminary assays in full time mode were performed as described in the Methods section (Fig. 6). The mean rate of dissociation of [^{3}H]NMS (k_{off}) and the mean half-life of dissociation ($t_{1/2}$) were calculated for each receptor subtype and their values are reported in Table 2.

Since [^{3}H]NMS dissociation was found to follow a monoexponential time course, a one point kinetic protocol was applied [28]. The residual binding of [^{3}H]NMS at only one time point was measured in the absence and presence of different concentrations of putative allosteric ligands and a single-point estimate of [^{3}H]NMS (k_{off}) was determined.

The incubation times necessary to equilibrate [^{3}H]NMS binding to all five muscarinic subtypes in the presence of an allosteric modulator were calculated around 2–3 times the estimated half-lives reported in Table 2: 80 min (hM_1), 20 min (hM_2), 100 min (hM_3), 90 min (hM_4) and 70 min (hM_5). Gallamine, CCh and the synthesized compounds were tested at several concentrations (0.01–100 μM), to assess their potency in inhibiting the radioligand dissociation from the five receptor subtypes. Untransformed data were analyzed in order to obtain estimates of the affinity of an allosteric agent for the [^{3}H]NMS-occupied receptor ($\log K_{occ}$) in a single step. Representative graphs of the one point kinetic assay experiment for Gallamine and CCh (Fig. 7A and B, for hM_1 and hM_2 subtypes respectively) show the good fit to the experimental

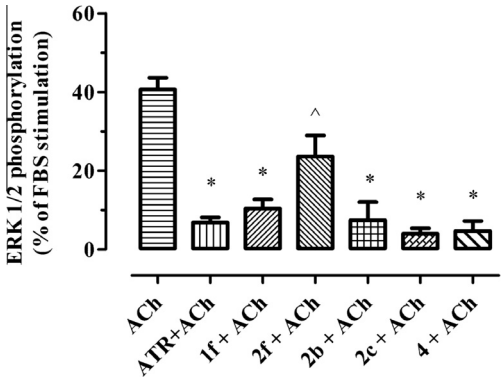

Fig. 5. Determination of ERK1/2 phosphorylation in intact cells stably transfected with hM_1 subtype receptors. Concentrations used are: ACh (10 nM), tested compounds (100 μM) and atropine (10 μM). Data are normalized to the response mediated by 10% serum and are presented as mean ± SEM of 3–6 experiments, each one performed in quadruplicate. Significantly different ($^*p \leq 0.0001$, $^\wedge p \leq 0.01$) from the control value ACh 10 nM.

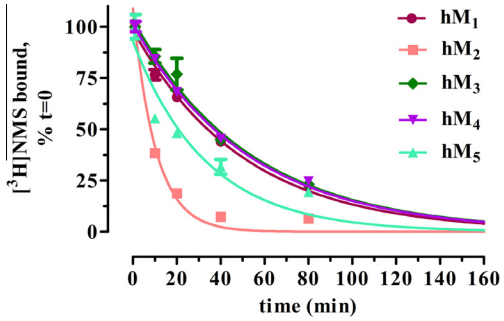

Fig. 6. Representative one point kinetic assay curves of the dissociation of [^{3}H]NMS (0.2 nM) from hM_{1-5} receptor subtypes. Re-association is blocked with an excess of atropine (10 μM). Data shown are the mean ± SEM from 3 to 11 experiments performed in duplicate.

data; the parameters obtained for all tested compounds are summarized in Table 3.

Like most other allosteric agents at muscarinic receptors, gallamine inhibited the dissociation of [^{3}H]NMS from all receptor subtypes almost completely and so gave rise to an increase in residual [^{3}H]NMS binding at the given time point (Fig. 7). Log K_{occ} values are in good agreement with the literature, confirming the preference for hM_2 subtype ($\log K_{occ}$ 5.16 ± 0.06) [37]. The orthosteric agonist CCh was tested as negative control and, as expected, it didn't produce any effect on the dissociation of [^{3}H]NMS.

In general, all tested compounds, although with different and in some cases very low potency, are able to slow down the rate of dissociation of [^{3}H]NMS at all subtypes. Compounds **1b**–**e** and **2b**–**e** reveal higher $\log K_{occ}$ values for hM_1, hM_2 and hM_4 with respect to hM_3 and hM_5 subtypes. The affinity of the tested compounds for the occupied receptor increases with linker's elongation, this effect being more evident for the tertiary amines compared to the corresponding quaternary ammonium analogs (Fig. 8). On the contrary, **1f** and **2f**, both carrying a hexamethylene chain, display low affinity for the allosteric site at all five subtypes (Table 3), deviating from the trend shown in Fig. 8. In addition, also the monovalent molecules **3** and **4**, carrying only one carbachol unit, display a different behavior, presenting lower affinity for hM_1 compared to hM_2–hM_5 (Table 3).

3.5. Docking studies

To rationalize the results of binding and functional experiments, docking studies were performed on the recently resolved hM_2 structure in complex with the agonist iperoxo and the allosteric modulator LY2119620 [38], for both ammonium derivatives **2a**–**f** and ammines **1a**–**f** in the protonated form; since both classes interact in a similar way, only the methiodides are discussed here. In detail, the short-chain derivatives ($n = 3$ or 5) can assume two distinct binding modes.

In the first pose (as shown in Fig. 9A for **2a**, $n = 3$), the ligands are completely accommodated in the orthosteric cavity, where they stabilize the following set of interactions: (i) one ammonium head is engaged in the key ion-pairing with Asp103, reinforced by a set of charge transfer interactions with surrounding aromatic residues (e.g., Tyr80, Trp99, Tyr426, Tyr430); (ii) the two carbamate moieties elicit clear H-bonds with Tyr104, Ser107 and Tyr403 and (iii) the second ammonium head approaches Asn108, Phe195, Trp400, and Asn404. In the second binding mode, the ligands assume a central pose by which they contact both the orthosteric and the allosteric sites. Specifically, both ammonium heads are engaged in ion-pairs, one with Asp103 in the orthosteric cavity and the other with Glu172 and Glu175 in the allosteric site,

Table 2
Half-time dissociation ($t½$) of [^{3}H]NMS and rate constants of dissociation (k_{off}) observed at hM_{1-5} receptor subtypes. Values are the mean ± SEM derived from 3 to 11 experiments performed in duplicate.

	hM_1	hM_2	hM_3	hM_4	hM_5
$t½$ (min)	34.95 ± 1.98	7.09 ± 0.28	36.64 ± 0.64	36.43 ± 1.99	23.71 ± 3.13
k_{off} (min^{-1})	0.020 ± 0.001	0.098 ± 0.004	0.019 ± 0.000	0.019 ± 0.001	0.030 ± 0.004

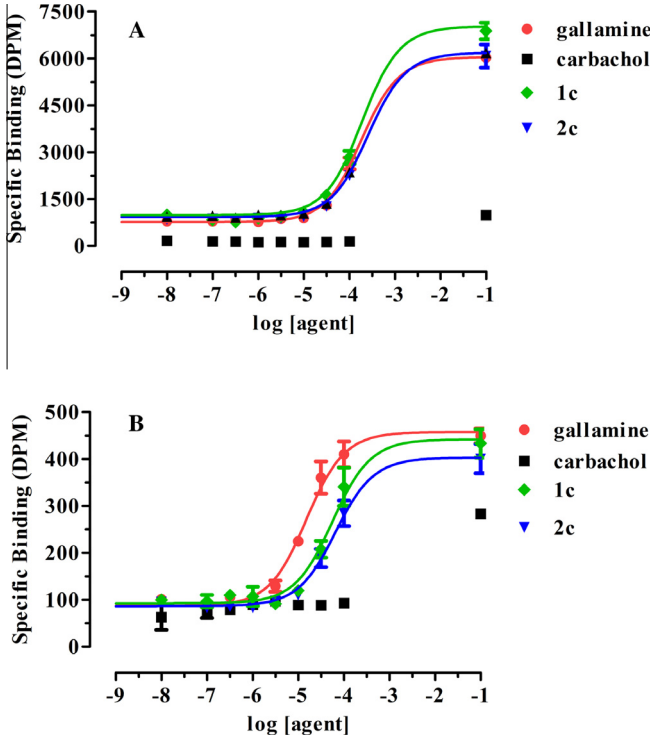

Fig. 7. Representative graphs of the one point kinetic assay for the determination of the affinity of the ligands gallamine and CCh at [^{3}H]NMS-occupied hM_1 (A) and hM_2 (B) receptor. These graphs show the increase in the [^{3}H]NMS bound to the receptor as the concentrations of the modulators increase. This is due to the reduction of the rate of the dissociation of [^{3}H]NMS. The range of concentrations used for the agents was 0.01–100 μM in addition of 10 μM of atropine. The data point at log[agent] = −1 represents the [^{3}H]NMS bound in the absence of added atropine and muscarinic ligand. The curves represent the non-linear square fits to the experimental data using an equation (Section 2.6) that estimates the affinity when the receptor is occupied by an orthosteric ligand.

the latter being further reinforced by charge transfer interactions with Tyr177. The two carbamate moieties elicit again H-bond interactions, but with Tyr426 and Asn419 in the orthosteric and the allosteric sites, respectively. For the short-chain derivatives, the first binding mode is markedly favored in terms of both calculated docking scores and relative abundance among the computed poses. This finding is in agreement with the affinity of these compounds which are comparable with that of carbachol thus underlining their incapacity to conveniently interact with both sites.

When extending the linker, the first binding mode becomes progressively less favored to disappear for $n = 6$ due to obvious steric hindrance. As exemplified in Fig. 9B for **2d** ($n = 9$), the long-chain analogs show only the second binding mode and assume a deeper pose compared to that shown by short-chain derivatives by which the dimethylaminoethylcarbamate moiety within the orthosteric cavity contacts Asn404 while retaining the already mentioned interactions with Asp103 plus the surrounding aromatic residues. The interactions established by the second carbachol unit, accommodated in the allosteric site, are similar to those already seen for the short-chain analogs, consisting in ion pairing between the ammonium moiety and Glu172 and Glu175, reinforced by a set of H-bonds with Tyr83, Tyr177, Asn419. However, it is worth noting that all derivatives, when assuming this second binding mode, are unable to insert the carbachol unit into the orthosteric cavity in a pose comparable to that shown by CCh: as a matter of fact, the linker constrains the dimethylaminoethylcarbamate moiety in an inverted arrangement which prevents the carbamate group to contact Asn404. In such a second binding mode the linker is inserted in a constrained channel lined by aromatic residues. Compounds **3** and **4**, endowed with only one carbachol moiety, insert it into the orthosteric site where it stabilizes the same interactions previously described for long-chain derivatives while the alkyl chain reaches the allosteric site where it can at most establish hydrophobic contacts. Taken together, these results can provide an explanation for the antagonistic

Table 3
Log affinity values ($\log K_{occ}$) for the tested compounds for the [^{3}H]NMS-occupied muscarinic receptors obtained from elaboration with Eq. (2) of experimental data. Values are reported as mean ± SEM of at least three experiments performed in duplicate. (ND, not detectable).

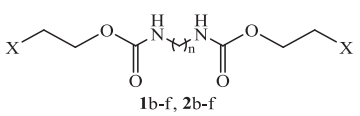

1b-f, **2**b-f

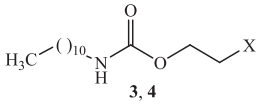

3, **4**

	n	X	hM_1	hM_2	hM_3	hM_4	hM_5
1b	5	NMe_2	3.43 ± 0.05	3.71 ± 0.11	3.36 ± 0.10	3.36 ± 0.14	3.39 ± 0.09
2b	5	NMe_3I	4.04 ± 0.03	4.64 ± 0.05	3.58 ± 0.15	4.34 ± 0.05	3.41 ± 0.11
1c	7	NMe_2	4.24 ± 0.07	4.57 ± 0.09	3.73 ± 0.09	4.14 ± 0.03	3.69 ± 0.05
2c	7	NMe_3I	4.11 ± 0.05	4.62 ± 0.07	3.71 ± 0.10	4.15 ± 0.04	3.53 ± 0.10
1d	9	NMe_2	5.00 ± 0.09	4.76 ± 0.05	4.14 ± 0.04	5.54 ± 0.16	3.94 ± 0.08
2d	9	NMe_3I	5.25 ± 0.12	4.98 ± 0.10	4.34 ± 0.02	5.36 ± 0.14	4.31 ± 0.03
1e	11	NMe_2	5.05 ± 0.22	4.72 ± 0.11	3.43 ± 0.16	5.16 ± 0.25	3.76 ± 0.04
2e	11	NMe_3I	5.43 ± 0.08	5.12 ± 0.15	4.10 ± 0.07	5.50 ± 0.12	4.35 ± 0.03
1f	6	NMe_2	3.13 ± 0.14	3.00 ± 0.08	3.50 ± 0.07	3.00 ± 0.12	3.62 ± 0.04
2f	6	NMe_3I	3.61 ± 0.06	3.95 ± 0.07	3.66 ± 0.04	3.58 ± 0.06	3.59 ± 0.08
3	–	NMe_2	3.92 ± 0.15	4.02 ± 0.17	4.19 ± 0.19	4.29 ± 0.08	4.27 ± 0.07
4	–	NMe_3I	3.84 ± 0.06	4.46 ± 0.09	4.40 ± 0.06	4.57 ± 0.15	4.40 ± 0.04
Gallamine			4.11 ± 0.06	5.16 ± 0.06	4.19 ± 0.06	4.56 ± 0.08	4.30 ± 0.07
Carbachol			ND	ND	ND	ND	ND

Please cite this article in press as: R. Matucci et al., Carbachol dimers as homobivalent modulators of muscarinic receptors, Biochem. Pharmacol. (2016), http://dx.doi.org/10.1016/j.bcp.2016.03.012

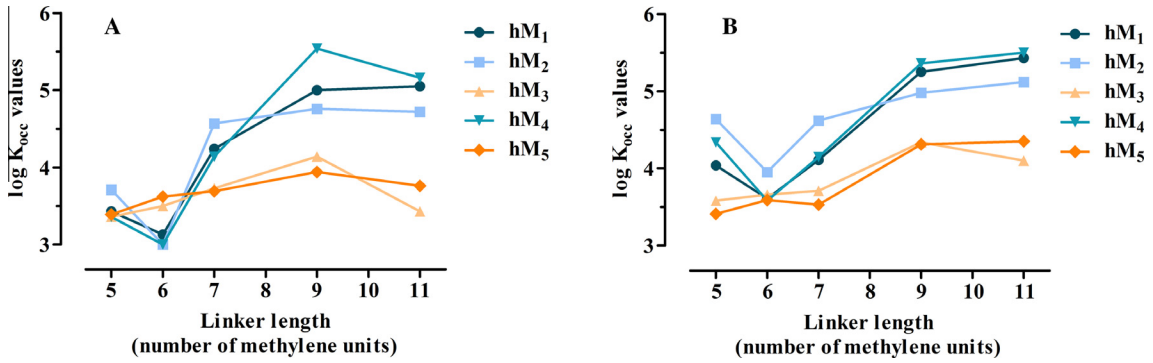

Fig. 8. Relationship between logK_{occ} values and linker's length. Connecting lines were drawn for hM_{1-5} mAChR to visualize trends (A, tertiary amines; B, quaternary ammonium compounds).

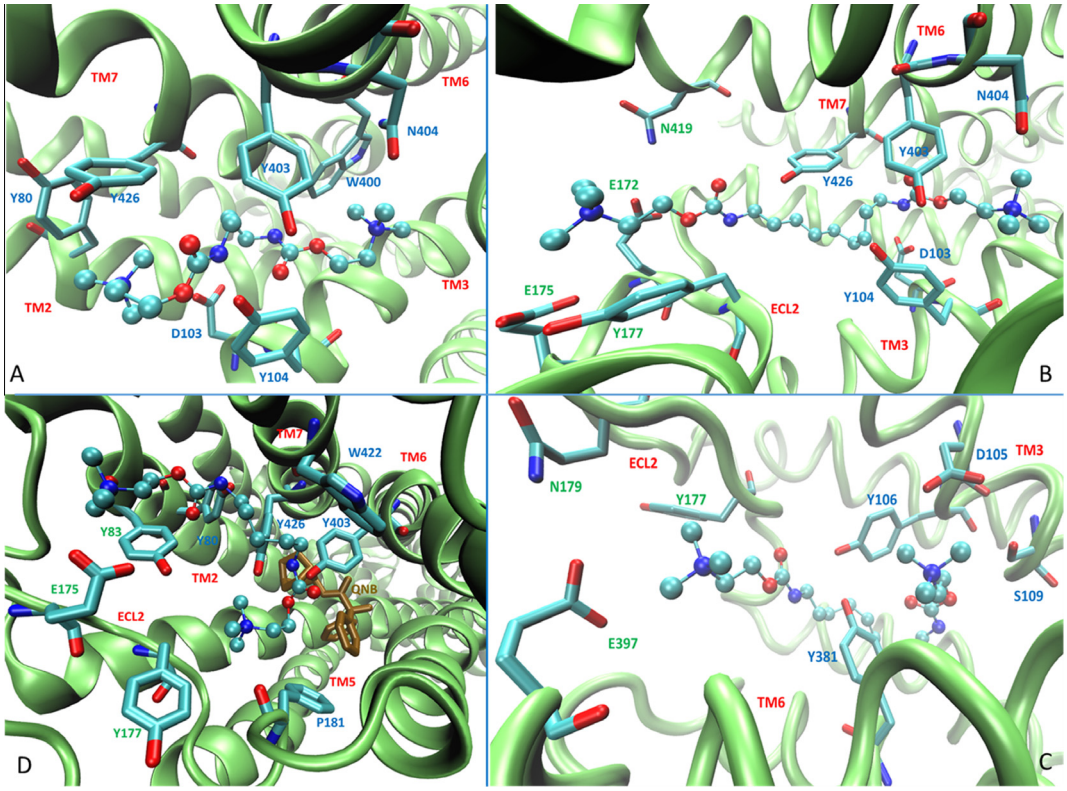

Fig. 9. Docking poses of selected ligands into the hM_1 and hM_2 receptors. A: **2a** ($n = 3$) within the orthosteric cavity of hM_2. B: **2d** ($n = 9$) docked between the orthosteric and allosteric sites of hM_2. C: **2d** docked between the orthosteric and allosteric sites of hM_1. D: **2b** ($n = 5$) into the allosteric site of the NMS-occupied hM_2 receptor.

activity of the long-chain derivatives, since they do achieve a rich interaction pattern while being unable to elicit the key contacts usually established by the agonists within the orthosteric site.

Since the compounds show higher affinity for the hM_1 receptor, compared to hM_2 subtype, docking simulations were also performed on a hM_1 homology model as generated using the above mentioned recently resolved hM_2 structure as the template. Also on this subtype, docking studies suggest significant differences on the binding mode of the compounds, depending on the length of the linker. In detail, the short-chain derivatives tend to remain in the allosteric site where one carbachol moiety elicits ionic interactions with Glu397 plus a set of H-bonds with Tyr85, Tyr179, Gln177, while the second carbachol group approaches the orthosteric site without reaching it. On the contrary, as exemplified by **2d** ($n = 9$) in Fig. 9C, the long-chain derivatives assume a central pose by which they occupy both the orthosteric and the allosteric sites. Such a pose brings to mind that previously described for the hM_2 subtype, although these ligands appear to be more fittingly accommodated in the hM_1 receptor. In fact, while the key contacts within the allosteric cavity are similar in both subtypes, the carbachol moiety within the orthosteric site assumes an optimal orientation being able to elicit the same key interactions established by CCh, namely the ammonium head with Asp105 plus the surrounding aromatic residues and the carbamate moiety with Asn382. Moreover the alkyl linker appears to be suitably inserted in a tight channel completely lined by aliphatic residues, which can form a rich set of apolar contacts with the ligand. Also on this subtype, compounds **3** and **4** show a binding mode similar to that of long-chain carbachol dimers, clearly lacking the polar contacts stabilized within the allosteric cavity.

Docking simulations were repeated using the M_2 resolved structure in complex with the QNB antagonist in order to mimic an experimental condition comparable with that experienced during kinetic binding studies. The obtained results reveal that all

compounds with two carbachol units are conveniently accommodated in the allosteric binding cavity regardless of the length of the linker. Thus Fig. 9D depicts the putative complex for **2b** ($n = 5$) which shows on hM_2 subtype the highest $\log K_{occ}$ value. The ligand is completely harbored in the allosteric site where it can elicit a rich set of polar contacts. In detail, (i) one ammonium head is engaged in the key ion-pairing with Glu175 reinforced by charge transfer interactions with surrounding aromatic residues (e.g., Tyr83 and Tyr88); (ii) the second ammonium head elicits only charge transfer interactions with Tyr177 and Phe181; (iii) both carbamate moieties are involved in several H-bonds with Tyr80, Thr187, Tyr403, Asn419, Thr423, and Tyr426; (iv) the linker elicits hydrophobic contacts with Trp422. All examined ligands show a very similar binding mode, permitted by their folding degree which increases with the length of the linker. Notably, some tyrosine residues which normally belong to the orthosteric site (i.e. Tyr403 and Tyr426) are here slightly shifted due to the presence of the antagonist and can participate to the interaction in the allosteric site, thus suggesting that these aromatic residues act as a watershed to divide the two considered binding sites.

4. Discussion

In this paper we report the characterization of a series of divalent ligands carrying two carbachol units. It is well known that the agonist carbachol is not endowed with subtype selectivity, but only with a small preference for M_2/M_4 as shown by our equilibrium binding studies (Table 1) [26]. On the contrary, the binding profile of the carbachol homodimers reported in this study is completely changed: from equilibrium binding studies their affinity is higher for hM_1, hM_3 and hM_5 than for hM_2 and hM_4 with the exception of the "short" derivatives **1a**,**b** and **2a**,**b**. Affinity increases with the linker's length, suggesting a contribution by this moiety, probably by hydrophobic interactions. However, the increase in pK_i is not smooth, since a "jump" in the affinity values can be seen going from the compounds with $n \leqslant 5$ to those with $n \geqslant 7$. The difference in affinity depends on the receptor subtype and the presence of the amine/ammonium functionality: for example, the increase in affinity going from methiodides **2b** to **2c** varies from about 180 times in hM_2 subtype to more than 5000 times in hM_4 subtype. Moreover, differences are larger for methiodides **2b,c** compared to tertiary amines **1b,c**. This behavior may be explained by a change in the binding mode of the compounds, which allows a better fit within the receptor, as if, for instance, a gap could be bridged between the binding sites accommodating the two pharmacophoric units. Indeed, docking simulations, performed on the recently resolved hM_2 structure [38], revealed significant differences between the simulated compounds depending on the length of their linker, suggesting a change in binding mode for $n = 6$. While short compounds ($n \leqslant 5$) may interact within the orthosteric binding site or between the orthosteric and allosteric sites, by increasing the length of the linker only the bitopic interaction is possible due to steric hindrance.

The comparison of the docking results obtained for hM_1 and hM_2 allows some considerations which correlate with the outcomes of equilibrium binding studies. First, in both receptors the binding mode depends on the length of the linker and only the long-chain analogs are able to occupy both binding sites. Second, the short-chain derivatives reveal significant differences between the two receptor subtypes: in fact, when docked on hM_2 receptor they tend to be completely harbored within the orthosteric site while on the hM_1 subtype they remain in the allosteric cavity. This different behavior is easily explained by considering that the hM_2 orthosteric pocket is larger and more flexible than the one in hM_1, as demonstrated by previous studies [39]. Third, while assuming comparable pose, the long-chain derivatives are predicted to elicit a more favorable pattern of interactions with hM_1 receptors compared to hM_2. This difference is due to the contacts established by the carbachol moiety within the orthosteric site as well as to the hydrophobic interactions stabilized by the linker.

Functional studies have shown that carbachol dimers have lost the muscarinic agonist properties of the parent compound. In fact, although some compounds were able to induce a contraction on guinea-pig ileum, this effect was not prevented by atropine, but it was blocked by hexamethonium, pointing to an involvement of the ganglionic nicotinic receptor. This agonistic activity on nicotinic receptor could be in a way expected since CCh is able to activate both muscarinic and nicotinic receptor, although, surprisingly, we found in the literature that compound **2f** ($n = 6$) and its congeners with general formula A (Fig. 1) and $n = 4$, 8, 10 have been described as neuromuscular blocking agents with no ganglionic stimulating activity [24,40]. To avoid interference with nicotinic activity, the functional properties of selected compounds (**1f**, **2b**, **2c**, **2f** and **4**) were tested for their ability to increase ERK1/2 phosphorylation in CHO cells, transfected with muscarinic receptors. All the tested compounds were found unable to activate the hM_1, hM_2 and hM_3 muscarinic receptors, while **2b**, **2c**, **2f** and **4** were able to prevent the increase in ERK1/2 phosphorylation induced by ACh. The different docking behavior can suggest a possible explanation, since the compounds fit into the muscarinic receptor binding site without eliciting the same pattern of interaction usually established by agonists within the orthosteric site.

The possible interaction with the allosteric site, suggested by the docking approach, is supported by the kinetic binding experiments: compounds **1b**–**e** and **2b**–**e** slow the dissociation rate of [^{3}H]NMS from the five muscarinic receptors; $\log K_{occ}$ values, calculated according to [28] were mostly in the same range as gallamine. With respect to equilibrium binding studies, a different preference is evidenced: higher affinity is usually found for the [^{3}H]NMS-occupied hM_2/hM_4 receptors, and also on hM1 for compounds **1d**,**e** and **2d**,**e**, with respect to hM_3/hM_5. The hexamethylene derivatives **1f** and **2f** display very low affinity for the allosteric site, as well as the "short" amine **1b**. As far as the undecyl derivatives **3** and **4** are concerned, the different trend of their $\log K_{occ}$ values suggest a different binding mode; in addition, their lower affinity for the [^{3}H]NMS-occupied hM_1 and hM_2 receptors, compared to that of the long dimers **1d,e** and **2d,e** ($n = 9$, 11, i.e. with the length of the linker approaching that of the undecyl residue), suggests an active role of the second carbachol unit in the interaction with the allosteric site.

In conclusion, we have prepared a series of homodimers of the well-known cholinergic agonist carbachol. The compounds have been analyzed by means of equilibrium and kinetic binding studies; docking simulations on the hM_1 and hM_2 receptors give a sound rationalization of the experimental data. Functional experiments show that homodimerization, connecting two carbachol units through the carbamic nitrogen atoms, gave derivatives which lost agonistic activity. Studies are ongoing on other carbachol homodimers, where the two units are linked in a different way, to further explore the structural requirements to bridge the orthosteric and allosteric binding sites.

Acknowledgments

This work was supported by grants from MIUR – Italy (PRIN 2009, 2009ESXPT2_002). We thank professor Fulvio Gualtieri for helpful discussion. This work is dedicated to our dear colleague Serena Scapecchi, who began this research but departed this life too early.

Please cite this article in press as: R. Matucci et al., Carbachol dimers as homobivalent modulators of muscarinic receptors, Biochem. Pharmacol. (2016), http://dx.doi.org/10.1016/j.bcp.2016.03.012

References

[1] J. Wess, R.M. Eglen, D. Gautam, Muscarinic acetylcholine receptors: mutant mice provide new insights for drug development, Nat. Rev. Drug Discov. 6 (2007) 721–733.
[2] A.C. Kruse, B.K. Kobilka, D. Gautam, P.M. Sexton, A. Christopoulos, J. Wess, Muscarinic acetylcholine receptors: novel opportunities for drug development, Nat. Rev. Drug Discov. 13 (2014) 549–560.
[3] N.C. Bodick, W.W. Offen, A.I. Levey, N.R. Cutler, S.G. Gauthier, A. Satlin, H.E. Shannon, G.D. Tollefson, K. Rasmussen, F.P. Bymaster, D.J. Hurley, W.Z. Potter, S.M. Paul, Effects of Xanomeline, a selective muscarinic receptor agonist, on cognitive function and behavioral symptoms in Alzheimer Disease, Arch. Neurol. 54 (1997) 465–473.
[4] N.R. Mirza, D. Peters, R.G. Sparks, Xanomeline and the antipsychotic potential of muscarinic receptor subtype selective agonists, CNS Drug Rev. 9 (2003) 159–186.
[5] P.J. Conn, C.K. Jones, C.W. Lindsley, Subtype-selective allosteric modulators of muscarinic receptors for the treatment of CNS disorders, Trends Pharmacol. Sci. 30 (2009) 148–155.
[6] B.J. Melancon, C.R. Hopkins, M.R. Wood, K.A. Emmitte, C.M. Niswender, A. Christopoulos, P.J. Conn, C.W. Lindsley, Allosteric modulation of seven transmembrane spanning receptors: theory, practice, and opportunities for central nervous system drug discovery, J. Med. Chem. 55 (2012) 1445–1464.
[7] K. Mohr, J. Schmitz, R. Schrage, C. Tränkle, U. Holzgrabe, Molecular alliance—from orthosteric and allosteric ligands to dualsteric/bitopic agonists at G protein coupled receptors, Angew. Chem. Int. Ed. 52 (2013) 508–516.
[8] K. Mohr, C. Tränkle, E. Kostenis, E. Barocelli, M. De Amici, U. Holzgrabe, Rational design of dualsteric GPCR ligands: quests and promise, Br. J. Pharmacol. 159 (2010) 997–1008.
[9] C. Valant, J. Robert Lane, P.M. Sexton, A. Christopoulos, The best of both worlds? Bitopic orthosteric/allosteric ligands of G protein-coupled receptors, Annu. Rev. Pharmacol. Toxicol. 52 (2012) 153–178.
[10] C. Valant, P.M. Sexton, A. Christopoulos, Orthosteric/allosteric bitopic ligands: going hybrid at GPCRs, Mol. Interv. 9 (2009) 125–135.
[11] P.S. Portoghese, From models to molecules: opioid receptor dimers, bivalent ligands, and selective opioid receptor probes, J. Med. Chem. 44 (2001) 2259–2269.
[12] T. Steinfeld, M. Mammen, J.A.M. Smith, R.D. Wilson, J.R. Jasper, A novel multivalent ligand that bridges the allosteric and orthosteric binding sites of the M_2 muscarinic receptor, Mol. Pharmacol. 72 (2007) 291–302.
[13] A. Bock, N. Mertem, R. Schrage, C. Dallanoce, J. Bätz, J. Klöckner, J. Schmitz, C. Matera, K. Simon, A. Kebig, L. Peters, A. Müller, J. Schrobang-Ley, C. Tränkle, C. Hoffmann, M. De Amici, U. Holzgrabe, E. Kostenis, K. Mohr, The allosteric vestibule of a seven transmembrane helical receptor controls G-protein coupling, Nat. Commun. 3 (2012) 1044.
[14] J.R. Lane, P. Donthamsetti, J. Shonberg, C.J. Draper-Joyce, S. Dentry, M. Michino, L. Shi, L. López, P.J. Scammells, B. Capuano, P.M. Sexton, J.A. Javitch, A. Christopoulos, A new mechanism of allostery in a G protein-coupled receptor dimer, Nat. Chem. Biol. 10 (2014) 745–752.
[15] C. Melchiorre, A. Cassinelli, W. Quaglia, Differential blockade of muscarinic receptor subtypes by polymethylene tetraamines. Novel class of selective antagonists of cardiac M_2 muscarinic receptors, J. Med. Chem. 30 (1987) 201–204.
[16] C. Melchiorre, A. Minarini, P. Angeli, D. Giardinà, U. Gulini, W. Quaglia, Polymethylene tetraamines as muscarinic receptor probes, Trends Pharmacol. Sci. 10 (Suppl.) (1989) 55–59.
[17] A. Christopoulos, M.K.O. Grant, N. Ayoubzadeh, O.N. Kim, P. Sauerberg, L. Jeppesen, E.E. El-Fakahany, Synthesis and pharmacological evaluation of dimeric muscarinic acetylcholine receptor agonists, J. Pharmacol. Exp. Ther. 298 (2001) 1260–1268.
[18] W.G. Rajeswaran, Y. Cao, X.-P. Huang, M.E. Wroblewski, T. Colclough, S. Lee, F. Liu, P.I. Nagy, J. Ellis, B.A. Levine, K.H. Nocka, W.S. Messer, Design, synthesis, and biological characterization of bivalent 1-methyl-1,2,5,6-tetrahydropyridyl-1,2,5-thiadiazole derivatives as selective muscarinic agonists, J. Med. Chem. 44 (2001) 4563–4576.
[19] U. Moser, C. Gubitz, M. Galvan, A. Immel-Sehr, G. Lambrecht, E. Mutschler, Aliphatic and heterocyclic analogues of arecaidine propargyl ester. Structure–activity relationships of mono- and bivalent ligands at muscarinic M_1 (M_4), M_2 and M_3 receptor subtypes, Arzneimittelforschung 45 (1995) 449–455.
[20] T. Disingrini, M. Muth, C. Dallanoce, E. Barocelli, S. Bertoni, K. Kellershohn, K. Mohr, M. De Amici, U. Holzgrabe, Design, synthesis, and action of oxotremorine-related hybrid-type allosteric modulators of muscarinic acetylcholine receptors, J. Med. Chem. 49 (2006) 366–372.
[21] J. Antony, K. Kellershohn, M. Mohr-Andrä, A. Kebig, S. Prilla, M. Muth, E. Heller, T. Disingrini, C. Dallanoce, S. Bertoni, J. Schrobang, C. Tränkle, E. Kostenis, A. Christopoulos, H.-D. Höltje, E. Barocelli, M. De Amici, U. Holzgrabe, K. Mohr, Dualsteric GPCR targeting: a novel route to binding and signaling pathway selectivity, FASEB J. 23 (2009) 442–450.
[22] I. Baracu, E. Tarnauceanu, I. Niculescu-Duvaz, Potential anticancer agents. XIII. Synthesis of new aliphatic and cycloaliphatic N-nitrosoureas, Rev. Roum. Chim. 22 (1977) 885–898.
[23] C. King, Cyclopolymerization of aliphatic 1,2-diisocyanates, J. Am. Chem. Soc. 86 (1964) 437–440.
[24] O. Schmid, L. Bilek, W. Seifred, Process for making bis-carbamic acid esters compounds, US2878279, 1959.
[25] R. Delaby, R. Hazard, J. Cheymol, P. Chabrier, H. Nayer, Di-uretane et leur preparation, FR1173901, 1953.
[26] S. Dei, P. Angeli, C. Bellucci, M. Buccioni, F. Gualtieri, G. Marucci, D. Manetti, R. Matucci, M.N. Romanelli, S. Scapecchi, E. Teodori, Muscarinic subtype affinity and functional activity profile of 1-methyl-2-(2-methyl-1,3-dioxolan-4-yl) pyrrolidine and 1-methyl-2-(2-methyl-1,3-oxathiolan-5-yl)pyrrolidine derivatives, Biochem. Pharmacol. 69 (2005) 1637–1645.
[27] M.M. Bradford, A rapid and sensitive method for quantitation of microgram quantities of protein, utilizing the principle of protein–dye binding, Anal. Biochem. 72 (1976) 248–253.
[28] S. Lazareno, N.J. Birdsall, Detection, quantitation, and verification of allosteric interactions of agents with labeled and unlabeled ligands at G protein-coupled receptors: interactions of strychnine and acetylcholine at muscarinic receptors, Mol. Pharmacol. 48 (1995) 362–378.
[29] M.A. Martí-Renom, A.C. Stuart, A. Fiser, R. Sánchez, F. Melo, A. Šali, Comparative protein structure modeling of genes and genomes, Annu. Rev. Biophys. Biomol. Struct. 29 (2000) 291–325.
[30] A. Pedretti, L. Villa, G. Vistoli, VEGA: a versatile program to convert, handle and visualize molecular structure on Windows-based PCs, J. Mol. Graph. Model. 21 (2002) 47–49.
[31] O. Korb, T. Stützle, T.E. Exner, Empirical scoring functions for advanced protein–ligand docking with PLANTS, J. Chem. Inf. Model. 49 (2009) 84–96.
[32] J.M. Van Rossum, Cumulative dose–response curves. Technique for the making of dose–response curves in isolated organs and evaluation of drug parameters, Arch. Int. Pharmacodyn. Ther. 143 (1963) 299–330.
[33] S. Scapecchi, E. Martini, C. Bellucci, M. Buccioni, S. Dei, L. Guandalini, D. Manetti, C. Martelli, G. Marucci, R. Matucci, Molecular modulation of muscarinic antagonists. Synthesis and affinity profile of 2,2-diphenyl-2-ethylthio-acetic acid esters designed to probe the binding site cavity, Farmaco 59 (2004) 971–980.
[34] R.U. Clague, R.M. Eglen, A.C. Strachan, R.L. Whiting, Action of agonists and antagonists at muscarinic receptors present on ileum and atria in vitro, Br. J. Pharmacol. 86 (1985) 163–170.
[35] E. Barocelli, V. Ballabeni, S. Bertoni, C. Silva, M. Impicciatore, Interactions of new and conventional H_3-antagonists with non-histaminergic receptors involved in neurogenic and myogenic contractile responses of guinea-pig ileum, J. Auton. Pharmacol. 19 (1999) 7–17.
[36] L.T. May, V.A. Avlani, C.J. Langmead, H.J. Herdon, M.D. Wood, P.M. Sexton, A. Christopoulos, Structure-function studies of allosteric agonism at M_2 muscarinic acetylcholine receptors, Mol. Pharmacol. 72 (2007) 463–476.
[37] A.L. Gnagey, M. Seidenberg, J. Ellis, Site-directed mutagenesis reveals two epitopes involved in the subtype selectivity of the allosteric interactions of gallamine at muscarinic acetylcholine receptors, Mol. Pharmacol. 56 (1999) 1245–1253.
[38] A.C. Kruse, A.M. Ring, A. Manglik, J. Hu, K. Hu, K. Eitel, H. Hubner, E. Pardon, C. Valant, P.M. Sexton, A. Christopoulos, C.C. Felder, P. Gmeiner, J. Steyaert, W.I. Weis, K.C. Garcia, J. Wess, B.K. Kobilka, Activation and allosteric modulation of a muscarinic acetylcholine receptor, Nature 504 (2013) 101–106.
[39] G. Vistoli, A. Pedretti, B. Testa, R. Matucci, The conformational and property space of acetylcholine bound to muscarinic receptors: an entropy component accounts for the subtype selectivity of acetylcholine, Arch. Biochem. Biophys. 464 (2007) 112–121.
[40] A.F. Danilov, I.J. Kvitko, V.V. Lavrentieva, M.J. Michelson, B.A. Porai-Koshits, E.A. Rozhkova, S.A. Shelkovnikov, Action of some bisquaternary derivatives of phthalic acids and related substances on neuromuscular transmission, Br. J. Pharmacol. 44 (1972) 765–778.

Please cite this article in press as: R. Matucci et al., Carbachol dimers as homobivalent modulators of muscarinic receptors, Biochem. Pharmacol. (2016), http://dx.doi.org/10.1016/j.bcp.2016.03.012